Available online at www.sciencedirect.com

SCIENCE DIRECT®

International Journal of Heat and Mass Transfer 48 (2005) 3402–3410

International Journal of HEAT and MASS TRANSFER

www.elsevier.com/locate/ijhmt

Sensitivity study for the mass transfer at a single droplet

A.R. Paschedag *, W.H. Piarah, M. Kraume

Institute of Chemical Engineering, Technische Universität Berlin, 10623 Berlin, Germany

Received 7 October 2003; received in revised form 26 November 2004
Available online 19 April 2005

Abstract

The mass transfer between a single droplet and a surrounding fluid can be described mathematically solving the momentum and mass balances in both phases (conjugate problem). This study of dimensionless parameters shows how the process is influenced by changes in material properties and operating conditions.

The influence of the Reynolds number *Re* on the mass transfer is found to be small and to vanish for creeping flows. A sensitivity to the viscosity ratio μ^* exists only in a limited range. The influence of the Peclet number *Pe* can be approximated for small *Pe* by considering only the external problem and for high *Pe* by considering only the internal problem.

Keywords: Mass transfer; Droplet; Two phase flow; Moving boundaries; Computational fluid dynamics

---

1. Introduction

Unsteady mass transfer between fluid particles and a surrounding continuous fluid is fundamental for many technical applications, like bubble columns, airlift reactors, liquid/liquid extraction, etc. This transport process is influenced by the physical properties of the species, by the operating conditions and by the particle properties.

To model this system mathematically the momentum and mass balance equations have to be solved in both phases considering adequate boundary conditions and interfacial conditions including all relevant forces and the thermodynamic equilibrium. At present, this can not be done in the full complexity because of two reasons: Firstly, the physics of some phenomena is not yet understood qualitatively and quantitatively, which leads to difficulties in setting up a mathematical description [16]. This includes changes in surface tension and surface mobility caused by the mass transfer process or irregular time dependent particle shapes.

The second point is the huge numerical effort required for a sufficiently accurate solution of the balance equations even for a single particle. For a swarm of particles the computing time will be in the order of weeks, months, or longer. To deal with this situation the mathematical description used in this work is based on a couple of simplifications: Only a single spherical droplet is considered and all effects caused either by changes of surface tension (like Marangoni convection) or by changes in the physical properties of the phases are neglected. Here, both phases are liquid, but the same algorithm can be applied also for liquid/gas and gas/liquid systems using suitable parameter sets. Based on the knowledge gained from this investigation the influence of parameter variations can be judged and suitable models for more complex systems can be developed in a subsequent step.

In our setup we investigate the mass transfer of an additive from a droplet into an ambient continuous

---

* Corresponding author. Tel.: +49 30 314 27825.
E-mail address: anja.paschedag@tu-berlin.de (A.R. Paschedag).

0017-9310/$ - see front matter © 2005 Elsevier Ltd. All rights reserved.
doi:10.1016/j.ijheatmasstransfer.2005.01.042

Nomenclature

A_i	area of interface, m^2
c	concentration, mol/m^3
D	diffusion coefficient, m^2/s
D^*	ratio of diffusion coefficients, –
d	diameter of the droplet, m
Fo	Fourier number, –
Fr	Froude number, –
$\vec{g}$	gravitational acceleration, m/s^2
k	mass transfer coefficient, m/s
m	distribution coefficient, –
$\dot{n}$	molar flux, mol/s
p	pressure, Pa
p'	reduced pressure, –
Pe	Peclet number, –
R	radius of the droplet, m
Re	Reynolds number, –
r	radial coordinate, m
r'	reduced radial coordinate, –
Re	Reynolds number, –
Sc	Schmidt number, –
Sh	Sherwood number, –
t	time, s
t'	reduced time, –
$\vec{v}$	velocity, m/s
$\vec{v}'$	reduced velocity, –
$\vec{v}_r$	relative velocity between the phases, m/s
Greek symbols	
μ	dynamic viscosity, kg/ms
μ^*	ratio of dynamic viscosities, –
ν	kinematic viscosity, m^2/s
ρ	density, kg/m^3
ρ^*	ratio of densities, –
ξ	averaged reduced concentration in the particle, –
ξ'	reduced concentration, –
Subscripts	
∞	far away from the droplet or after long time
0	initial
1	dispersed phase
2	continuous phase
i	interface

liquid phase. Mass transfer in the opposite direction can be described similarly. The initial additive concentration in the continuous phase is zero which is an easy but not restricting assumption since mass transfer and the Sherwood number used for its description depend only on concentration differences and not on absolute concentrations.

Mass transfer around a single droplet has been studied experimentally and numerically by a number of research groups during the last decades. The activities in this field served on the one hand to the validation of numerical methods by comparing the results to analytical solutions of limiting cases (e.g. [3]), and on the other hand they were used to validate models with respect to experimental data (e.g. [17]). In the first case good agreement was found up to Peclet numbers of 10^4 [12]. In the second case most simulations resulted in slower mass transfers than found in the corresponding experiments. Computations with advanced models describing the interfacial processes have not yet been presented. Simple models like those that involve an artificial increase of the diffusion coefficient D [5,6] are not investigated in this paper since the dependence of the modified diffusion coefficient D on material or flow properties is not known and thus the prediction reliability of such models is not higher compared to the basic model. However, since this paper gives mainly a parameter study in terms of dimensionless numbers the solution for such adapted models can be obtained by replacing the molecular diffusion coefficient by a modified one that is expressed in these dimensionless numbers.

There are a couple of parameters describing fluid properties of the two phases that influence the mass transfer between them. The influence of the ratio of these parameters can be studied. The goal of the present paper is not a general description of the influence of parameters on the system behavior but determination of the range in which a parameter has an influence and the one in which it can be varied without affecting the resulting asymptotic Sherwood number Sh_∞. Sh_∞ is a dimensionless measure for the mass transfer rate. The investigations will concentrate on the Reynolds number Re, the Peclet number Pe, and the viscosity ratio μ^*. From these, regions of stability against changes in the operating condition and of sensitivity to operating conditions can be derived. Correspondingly, ranges of parameters can be found in which changes of operating conditions do not influence Sh_∞ and ranges in which they do.

2. Model description

2.1. Velocity field

Under the assumptions discussed in Section 1 the velocity field $\vec{v}$ inside and outside the droplet can be considered to be stationary and independent of the concentration field. It can be computed solving the continuity equation and the Navier–Stokes equation

$$0 = \nabla \cdot \vec{v} \tag{1}$$

$$\frac{\partial \vec{v}}{\partial t} = 0 = -(\vec{v} \cdot \nabla)\vec{v} + \nu(\Delta \vec{v}) - \frac{1}{\rho}\nabla p + \vec{g} \tag{2}$$

for each phase. (All equations are given here in their dimensional form. The complete set of dimensionless equations is shown in Appendix A.) The outer boundary conditions have to be chosen in a way that an infinite fluid of uniform state is approximated with only minimal disturbance by the droplet. Therefore, the diameter of the simulated domain is by a factor of 100 larger than the droplet. The main flow velocity is determined at all outer boundaries apart from the outlet face. Since the droplet itself is considered to be stationary, this main flow velocity is equal to the relative velocity between droplet and continuous phase caused by differences in the density.

The interfacial conditions include equal velocities and shear stresses for both phases. Their mathematical formulations can be found in [14].

Two dimensionless numbers characterize the velocity field, Re and μ^*. The Reynolds number is determined by the relative velocity between the two phases $\vec{v}$ caused by density differences. It is calculated from the physical properties of the continuous phase (index 2): $Re = 2R \mid \vec{v}_r \mid \rho_2/\mu_2$ (see notation list for details). $Re < 0.1$ characterises a creeping flow. For higher Re wakes are formed behind the droplet, but the flow remains laminar for technical relevant cases ($Re < 500$). $\mu^* = \mu_1/\mu_2$ is the viscosity ratio of dispersed (index 1) and continuous phase. As a rough orientation one can consider $\mu^* < 10^{-2}$ representing bubbles in liquids, $0.1 < \mu^* < 10$ representing liquid/liquid systems and $\mu^* > 10^2$ representing drops in gases.

2.2. Concentration field

Based on the numerically determined velocity field the concentration field for the transferred component can be computed. The transient concentration distribution is determined by the mass balance equation:

$$\frac{\partial c}{\partial t} = -\vec{v} \cdot \nabla c + \nabla \cdot (D \nabla c) \tag{3}$$

which has to be solved for each phase. The outer boundaries of the continuous phase apart from the outlet are characterized by a constant concentration, in our case zero. The coupling at the interface can be described using the distribution coefficient m and the equality of molar fluxes $\dot{n}$ to and from the interface:

$$r = R, \quad 0 \leqslant \theta \leqslant \pi: \quad m = \frac{c_{1i}}{c_{2i}} \tag{4}$$

$$r = R, \quad 0 \leqslant \theta \leqslant \pi: \quad \dot{n}_{1i} = \dot{n}_{2i} \tag{5}$$

with c_{1i} and c_{2i} being the interfacial concentrations.

The most important parameter for the mass transfer is the Peclet number $Pe = 2R \mid \vec{v}_r \mid /D$. For the internal and the conjugate problem the diffusion coefficient of the dispersed phase D_1 is used while for the external problem the one for the continuous phase D_2 is used. Since for the conjugate problem in all cases discussed here the ratio of diffusion coefficients D^* is 1 the definition of Pe is the same for all cases considered and a comparison of the cases can be done. A similar problem occurs for the dimensionless presentation of time. Here the Fourier number $Fo = tD/R^2$ is applied with the analogous use of diffusion coefficients.

The thermodynamic equilibrium at the interface is described by the distribution coefficient $m = c_{1i}/c_{2i}$. Since the driving force for the mass transfer is directly proportional to m the effects of changes in m can be predicted and m shall not be considered in more detail here but taken to be 1 in all cases.

An obvious way to monitor the process over time in a dimensionless framework is to consider the dimensionless mean concentration in the droplet which is defined as

$$\xi(t) = \frac{(\overline{c_1}(t) - mc_{2\infty})}{(c_{10} - mc_{2\infty})} \tag{6}$$

whereby $\overline{c_1}$ is the mean concentration in the droplet, c_{10} is the initial concentration in the droplet and $c_{2\infty}$ is the concentration in the continuous phase far away from the droplet. ξ gives an impression which fraction of the originally available mass has been transferred between the phases at a certain time. More common in engineering is the description of the mass transfer efficiency using the time averaged mass transfer coefficient k and the appropriate dimensionless Sherwood number Sh derived from it:

$$k = \frac{\dot{n} \ln \dfrac{c_{10} - mc_{2\infty}}{\overline{c_1}(t) - mc_{2\infty}}}{A_i(c_{10} - \overline{c_1}(t))} \tag{7}$$

$$Sh = \frac{2kR}{D} \tag{8}$$

with A_i being the area of the interface and $\dot{n}$ the molar flux across it. In the present paper the results will be discussed based on the Sherwood number. An advantage of this representation is that the Sherwood number reaches a steady limit for large Fo, since the reduction in mass flow and driving concentration difference develop proportionally. This asymptotic value Sh_∞ is numerically very sensitive since it gives the ratio of small values. But the technical relevance of that asymptotic value depends on the concentration level at which it is reached. If at that time most of the mass transfer has taken place Sh_∞ is not characteristic for the process as a whole.

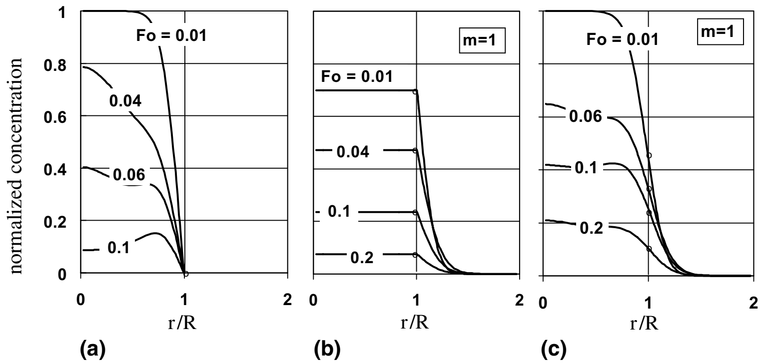

Fig. 1. Transient concentrations normalized by initial concentration in the particle for the different basic cases ($Re = 100$, $\mu^* = 1$, $Pe = 10^4$). (a) Internal problem, (b) external problem and (c) conjugate problem.

Even to solve Eqs. (3)–(5) coupled for both phases (conjugate problem) long computing times are required (in the range of some days on a single processor) and therefore many authors [2,8] reduce the problem size further by completely separating the mass transfer within the droplet (internal problem) from the mass transfer in the continuous phase (external problem). This is done assuming that the relevant mass transfer resistance in the complementary phase is negligible. The overall mass transfer coefficient of the entire problem is derived as a combination of the two separate mass transfer coefficients for each phase. The basic evolution of the reduced concentration field with time can be seen in Fig. 1 for the mass transfer of a component from a droplet to the ambient flow. The initial concentration outside the droplet is zero and the Reynolds number is 100.

An infinitely fast mass transfer in the continuous phase (internal problem) results in a constant concentration (in time and space) at the interface which is in thermodynamic equilibrium with the concentration far away from the droplet. The concentration is then given by the boundary conditions for the continuous phase. This is shown in Fig. 1(a).

An infinitely fast mass transfer inside the droplet results in a spatially uniform concentration inside the droplet that changes with time. Consequently, also the interfacial concentration which acts as boundary condition for the external problem is constant along the interface but varies with time (see Fig. 1(b)). The limits in validity of this assumption are discussed in [12].

Fig. 1(c) shows that for the conjugate problem the concentration profiles in both phases as well as at the interface are transient.

3. Numerical setup

As mentioned above the domain for the simulations has the 100-fold size of the droplet. The system can be assumed to be axially symmetric. Using this property the model area was reduced to a two dimensional slice. The domain is bounded by an inlet and an outlet perpendicular to the axis, a moving wall parallel to the axis and two symmetry planes. The fixed velocity and concentration at the inlet and the wall represent the state of the continuous phase undisturbed by the droplet. The interfacial conditions mentioned in Section 2 are introduced as moving wall boundary conditions for both phases by user coding.

The computations have been carried out using the commercial CFD code Star-CD. The code is based on finite volume discretization. While there are no special numerical requirements for the computation of the stationary velocity field the solution of the concentration field is sensitive to the grid properties, the discretization scheme, and the time step width. This gets especially important for high Peclet numbers where the influence of convective processes is strong compared to diffusive ones.

The grid consists of about 30000 cells, nearly 5000 of them are inside the droplet. For the discretization of convective terms a limited third order scheme (MARS) has been used and time is discretized using the Crank–Nicolson-method. The time step is adapted manually in relation to the progress of mass transfer in a way that $\Delta Fo = 10^{-6}$–10^{-5}.

4. Results

4.1. Influence of fluid dynamics

Firstly, we consider the internal problem. There are two limiting cases for the viscosity ratio μ^*. If the viscosity of the droplet is much higher than that of the continuous phase the droplet behaves like a solid particle. No significant internal circulation occurs and the mass transfer inside the droplet is only diffusive. This case occurs for liquid droplets in a gas. Fig. 2 shows that even for $\mu^* = 100$ these conditions are not completely fulfilled for the internal problem. This means that although the fluid dynamic behavior is comparable to that of a rigid sphere the influence of the internal circulation remains relevant for the mass transfer, especially at high *Pe*. From the plot of mean concentration versus *Fo* in Fig. 2 it is obvious that the deviation from the behavior of the rigid sphere starts at significantly high concentrations of about $\xi = 0.8$.

The second limiting case is $\mu^* < 1$. This means that the mobility inside the droplet is larger than the one of the surrounding fluid. Consequently, the interface follows the continuous phase and the circulation in the droplet becomes independent of a further decrease in μ_1. Fig. 2 shows that in the range $1 \leqslant \mu^* \leqslant 0.01$ the limiting case is reached. The comparison between Figs. 2 and 3 shows that the effect discussed for the mean concentration is also valid for the mean Sherwood number. Fast reduction of the concentration corresponds to large Sherwood numbers and while the concentration curves asymptotically approach zero the Sherwood number reaches a constant value.

In the case of the external problem a limit for high μ^* does not exist. The curves converge to the one for the solid particle, but a μ^* above which this limit is reached cannot be given. In the range $1 \leqslant \mu^* \leqslant 0.01$ a slight effect remains but it is no more significant (Fig. 4), so the limit can be considered similar to the internal problem.

For the conjugate problem (Fig. 5) the limit for low μ^* is also in this range. In principle the mass transfer is always slower for the conjugate problem than for the separate internal and external problems with the

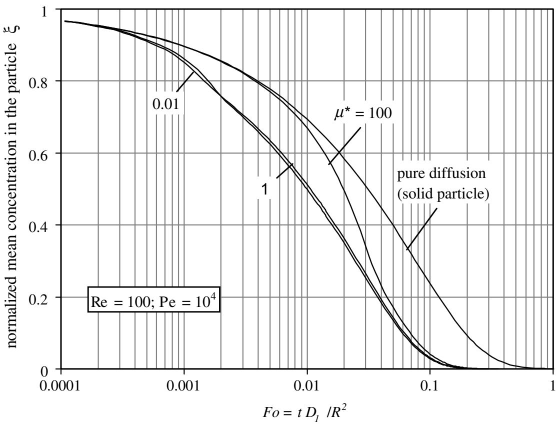

Fig. 2. Normalized concentration as a function of time for different μ^*, internal problem.

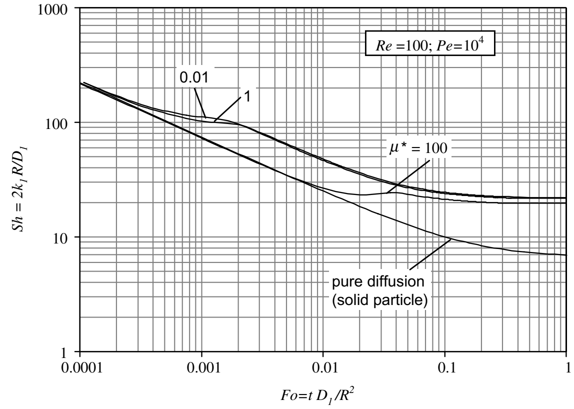

Fig. 3. Sherwood number as a function of time for different μ^*, internal problem.

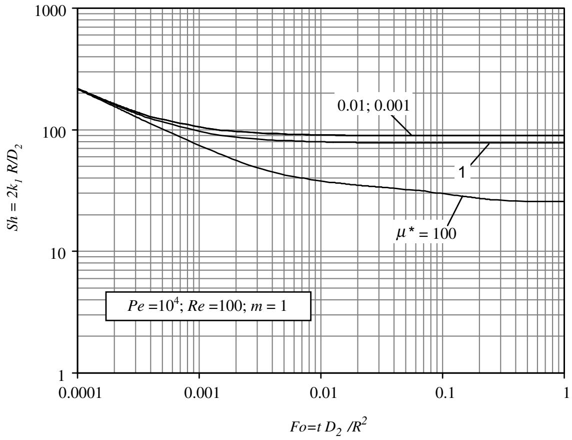

Fig. 4. Sherwood number as a function of time for different μ^*, external problem.

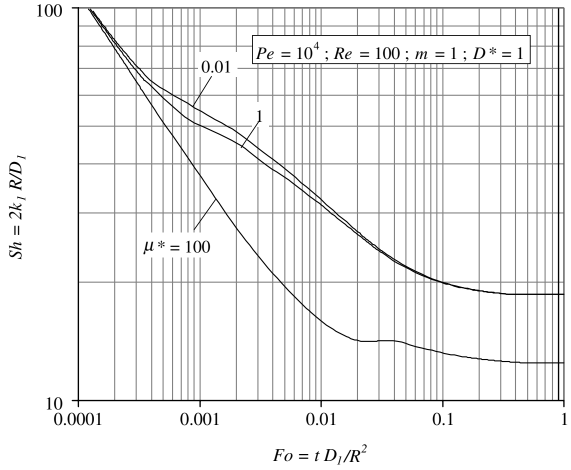

Fig. 5. Sherwood number as a function of time for different μ^*, conjugate problem.

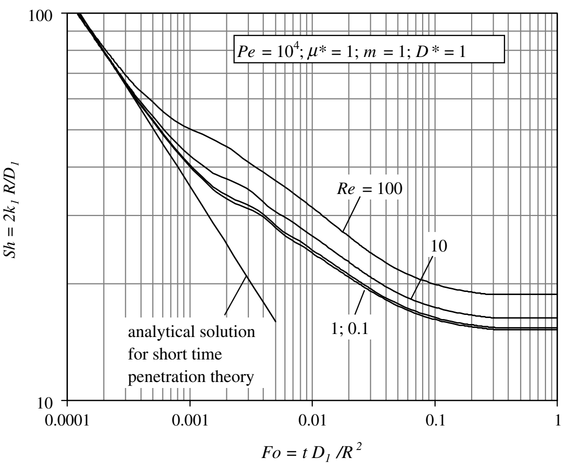

Fig. 6. Sherwood number as a function of time for different *Re*, conjugate problem.

same parameter set since there are mass transfer resistances in both phases instead of only one. Consequently, there exists no limit for high μ^* in the same sense as it does not exist for the external problem.

The influence of the Reynolds number in the range discussed is relatively small. This is shown for a representative parameter set for the conjugate problem in Fig. 6. For the external problem the effect is in the same range and for the internal problem it is even smaller. Furthermore, in the range of creeping flow ($Re < 0.1$) the effect of changes in *Re* vanishes completely [13]. This result has to be expected since in that range the molecular momentum transport is significant compared to convective momentum transport. Consequently, further decrease of convection has no effect on the mass transfer.

Even for larger Reynolds numbers with convective momentum transfer dominant to the molecular one the structure of the flow field remains mainly unchanged compared to smaller *Re* besides the formation of wakes behind the droplet. The stream lines outside the droplet are basically parallel to the interface in the region relevant for the mass transfer. This means that mass transfer from the interface is mainly diffusive and depends on the concentration gradient normal to the interface. This gradient changes at high Reynolds numbers slightly with increasing convective transport compared with molecular one but not by orders of magnitude. Inside the droplet the streamlines are elliptically closed. Due to the high velocity the concentration gradient along the streamlines is marginal compared to the one perpendicular to them and a further change in the velocity does not change the circumstances noticeably. As a result the only mechanism which accelerates the mass transfer at large *Re* is the change in the concentration gradient in the continuous phase and consequently, the influence on the external problem is stronger than on the internal problem. The small influence of changes in *Re* is parallel to the finding that small inaccuracies in the computation of the velocity field do not have a significant influence on the prediction of the mass transfer, as described e.g. in [14].

4.2. Influence of mass transfer

Mass transfer can be characterized by the Peclet number giving the ratio of convective and diffusive mass transfer. The influence of *Pe* shall be discussed first for the internal problem. In this case *Pe* describes the ratio between convection and diffusion inside the droplet, while the outer diffusion is infinitely fast. Fig. 7 shows how the reduced concentration profiles which are stationary at the end of the process change with *Pe*. It can be seen that there are the two limiting cases of diffusion determined system and convection determined system. For $Pe < 10$ the transport is similar to that in a particle without internal circulation because diffusion is dominant. Further increase in the diffusivity speeds up the mass transfer proportionally which leads to identical behavior of *Sh* over *Fo* (Fig. 8). The limit for the asymptotic Sherwood number $Sh_\infty = 6.58$ at $Pe = 0$

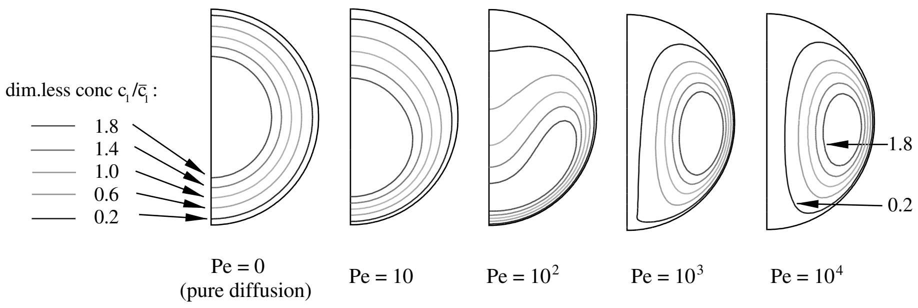

Fig. 7. Concentration profile for a long time (concentration normalized by actual mean concentration in the particle) for different *Pe*, internal problem, $Re = 100$, $\mu^* = 1$, flow upward.

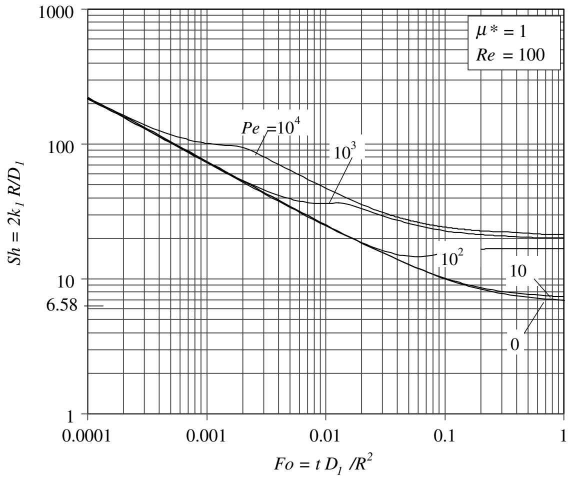

Fig. 8. Sherwood number as a function of time for different *Pe*, internal problem.

has been determined theoretically by Newman [10] for pure diffusion.

A second limit exists for high Peclet numbers. If the convective mass transfer dominates the diffusive one, the concentration along each streamline is nearly constant. Since the streamlines are in a wide range parallel to the interface the mass transfer to the interface is only due to diffusion. A further increase in speed of the convective transport does not influence the mass transfer significantly. Nevertheless, the Peclet number at which this situation is reached varies with the Reynolds number. A more general statement can be made using the Schmidt number ($Sc = Pe/Re = \nu/D$) which is a material constant instead of the Reynolds number. Fig. 9 shows, for different Peclet numbers and two different Schmidt numbers, the Fourier number at which 99% of the mass transfer has taken place. For both *Sc* the influence of *Pe* vanishes from about $Pe = 10^4$. This is discussed in more detail in [11].

An analytical solution of $Sc_\infty = 17.7$ is given for high *Pe* in the case of creeping flow by Kronig and Brink [8]. At higher Reynolds numbers the values of Sc_∞ are slightly higher as discussed above. This limiting case is even more relevant than the one at low *Pe* since for most practical applications *Pe* is in the range of 10^4–10^6.

For the external problem the situation is different. Since the streamlines are not closed, the mass transfer rate increases with the velocity as well as with the diffusivity. Consequently, the asymptotic Sherwood number increases proportionally to *Pe* (see Fig. 10). A limit exists only in the case of a droplet resting in the surrounding fluid, which means that there is no relative velocity. For this pure diffusive case the theoretical asymptotic value of *Sh* is 2 [15]. For the range of *Pe* considered ($10 \leqslant Pe \leqslant 10^5$) this results in a much wider range of asymptotic Sherwood numbers (more than two orders of magnitude) compared to the internal problem (less than one order of magnitude).

For the conjugate problem the effects inside and outside the droplet are relevant. In this case the values for *Sh* are always lower than for the internal as well as for the external problem as discussed for the viscosity ratio. Some resulting curves are shown in Fig. 11. As for the internal problem, there is a limit in Sh_∞ for high *Pe* and as for the external problem there is one for small *Pe*. But, for small *Pe* the computing time needed to determine Sh_∞ is very long and therefore simulations to determine this limit have not been carried out. In general, it is found that for small *Pe* the external problem is rate determining and for large *Pe* the internal problem (see also [7]).

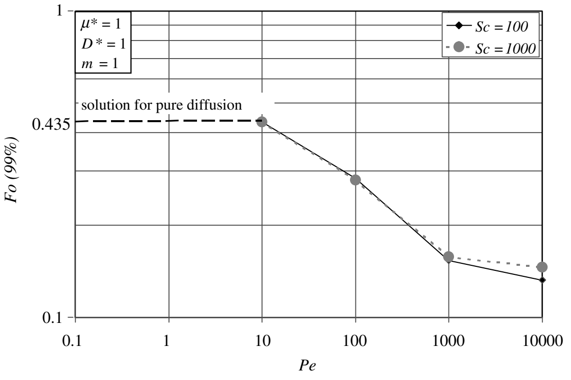

Fig. 9. Influence of *Pe* on the time for 99% mass transfer, internal problem.

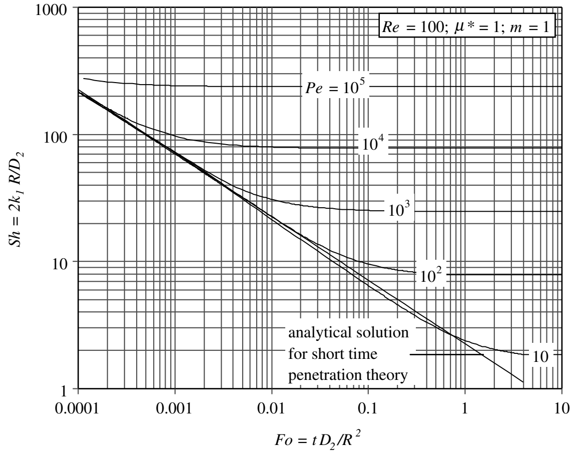

Fig. 10. Sherwood number as a function of time for different *Pe*, external problem.

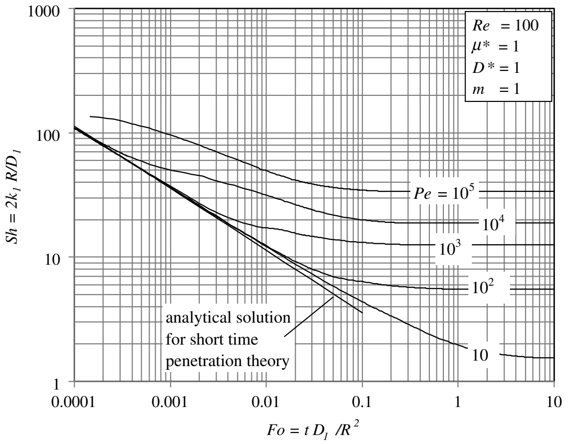

Fig. 11. Sherwood number as a function of time for different *Pe*, conjugate problem.

5. Conclusions

The mass transfer between a single droplet and an ambient liquid flow can be described systematically using dimensionless numbers. The parameters needed for a full characterization of a non-reacting system are *Re*, μ^*, *m*, D^* and *Pe*. Depending on the case (internal, external, conjugate problem) limits can be found, beyond which further changes of certain parameters do not influence the transport rate any more. In the range of sensitivity to the parameters the Sherwood number increases with *Re* and *Pe* and decreases with μ^*.

A variation of μ^* has a significant effect in the range between 0.1 and 100. Below that limit the interface moves with the same velocity as the surrounding fluid without slowing down it while above the droplet behaves similar to a rigid sphere.

A limit for the Reynolds number influence gives $Re = 1$, below which the viscous momentum transfer becomes dominant. For higher *Re* the influence of this parameter remains small which means, that there is no significant influence of the flow conditions on mass transfer as long as no additional disturbances like Marangoni convection occur.

For the variation of *Pe* an upper limit exists only for the internal problem. In that case, for $Pe \geqslant 10^4$ the concentration along each streamline is constant and mass transfer perpendicular to the streamlines and to the interface is only diffusive. Below $Pe = 10$ the problem is diffusion limited.

In general, for cases which are approximately internal problems the parameter range which influences the mass transfer rate is smaller than in the other cases and therefore, usually the precision of a priori guesses will be better.

Even if the conjugate problem cannot be described by defining the total mass transfer resistance as a sum of the resistances of the internal and the external problem, qualitatively the influence of a parameter can be gained from its influence on the internal and on the external problem. For low *Pe* the external problem is rate determining and the for large *Pe* the internal problem.

Acknowledgement

W.H. Piarah would like to thank the DAAD for the support of his work by a fellowship.

Appendix A. Dimensionless equations

For easier understanding the governing equations are given in dimensionless form here. Some additional definitions will be provided at the beginning to define all quantities properly. Slight modifications are required for the internal and the external problem where one of the diffusion coefficients is infinitely large and only one mass transfer equation is used. In the figures the results are presented in relation to the Fourier number instead of the dimensionless time defined below as most discussions on this topic use this form [1,4,9].

Definitions:

$$\begin{array}{ll}
t' = \dfrac{t \mid \vec{v}_r \mid}{d} = Fo\dfrac{Pe}{4} & \vec{v}' = \dfrac{\vec{v}}{\mid \vec{v}_r \mid} \\
r' = \dfrac{2r}{d} & p' = \dfrac{p}{\rho_1 \mid \vec{v}_r \mid^2} \\
\xi_1' = \dfrac{(c_1 - mc_{2\infty})}{(c_{10} - mc_{2\infty})} & \xi_2' = \dfrac{(c_2 - c_{2\infty})}{(c_{10}/m - c_{2\infty})} \\
\nabla' = \nabla d & \\
\mu^* = \dfrac{\mu_1}{\mu_2} & Re = \dfrac{d \mid \vec{v}_r \mid \rho_2}{\mu_2} \\
\rho^* = \dfrac{\rho_1}{\rho_2} & Pe = \dfrac{d \mid \vec{v}_r \mid}{D_1} \\
D^* = \dfrac{D_1}{D_2} & Fr = \dfrac{\mid \vec{v}_r \mid^2}{d \mid \vec{g} \mid}
\end{array} \tag{A.1}$$

Disperse phase:

$$\begin{aligned}
&0 = \nabla' \cdot \vec{v}' \\
&\frac{\partial \vec{v}'}{\partial t'} = 0 = -(\vec{v}' \cdot \nabla')\vec{v}' + \frac{\mu^*}{Re\,\rho^*}(\varDelta' \vec{v}') - \nabla' p' + \frac{1}{Fr} \\
&\frac{\partial \xi_1'}{\partial t'} = -\vec{v}' \cdot \nabla' \xi_1' + \frac{1}{Pe}\nabla' \cdot (\nabla' \xi_1')
\end{aligned} \tag{A.2}$$

Continuous phase:

$$\begin{aligned}
&0 = \nabla' \cdot \vec{v}' \\
&\frac{\partial \vec{v}'}{\partial t'} = 0 = -(\vec{v}' \cdot \nabla')\vec{v}' + \frac{1}{Re}(\varDelta' \vec{v}') - \rho^* \nabla' p' + \frac{1}{Fr} \\
&\frac{\partial \xi_2'}{\partial t'} = -\vec{v}' \cdot \nabla' \xi_2' + \frac{1}{PeD^*}\nabla' \cdot (\nabla' \xi_2')
\end{aligned} \tag{A.3}$$

Conditions at the interface:

$$\begin{aligned}
&v'_{r1} = v'_{r2} = 0\\
&v'_{\Theta 1} = v'_{\Theta 2}\\
&\mu^* \left(\frac{\partial v'_\Theta}{\partial r'} - \frac{v'_\Theta}{r'} \right)\Bigg|_1 = \left(\frac{\partial v'_\Theta}{\partial r'} - \frac{v'_\Theta}{r'} \right)\Bigg|_2\\
&\frac{\xi'_1}{\xi'_2} = 1\\
&D^* \frac{\partial \xi'_1}{\partial r'} = \frac{\partial \xi'_2}{\partial r'}
\end{aligned} \qquad \text{(A.4)}$$

References

[1] B. Brander, Impuls- und Stofftransport durch die Phasengrenzflache von kugelformigen fluiden Partikeln, Ph.D. Thesis, TU Berlin, 1993.

[2] H. Brauer, Particle/fluid transport process, Fortschr. Verfahrenstech. 17 (1979) 61–99.

[3] B.I. Brounshtein, A.S. Zheleznyak, G.A. Fishbein, Heat and mass transfer in interaction of spherical drops and gas bubbles with a liquid flow, Int. J. Heat Mass Transfer 13 (1970) 963.

[4] R. Clift, J.R. Grace, M.E. Weber, Bubbles, Drops and Particles, Academic Press, New York, 1978.

[5] E.A. Handlos, T. Baron, Mass and heat transfer from drops in liquid–liquid extraction, AIChE J. 3 (1) (1957) 127–136.

[6] M. Henschke, A. Pfennig, Mass-transfer enhancement in single-drop extraction experiments, AIChE J. 54 (10) (1999) 2079–2085.

[7] M. Kraume, A. Paschedag, W.H. Piarah, K. Schulze, Unsteady conjugate mass transfer in single drop systems, in: Proceedings of the 3rd European Congress of Chemical Engineering (ECCE), Nürnberg, Germany, 2001.

[8] R. Kronig, J.C. Brink, On the theory of extraction from falling drops, Appl. Sci. Res. A2 (1950) 142–154.

[9] H. Luo, H.F. Svendsen, Theoretical model for drop and bubble breakup in turbulent dispersions, AIChE J. 42/5 (1996) 1225–1233.

[10] A.B. Newman, The drying of porous solid, diffusion and surface emission effects, Trans. AIChE 27 (1931) 203.

[11] A. Paschedag, W.H. Piarah, M. Kraume, Unsteady mass transfer in single drop systems with interfacial mobility, in: B. Sarler, C.A. Brebbia (Eds.), Moving Boundaries VI, WIT Press, Southampton, 2001, pp. 195–204.

[12] A. Paschedag, W.H. Piarah, M. Kraume, Grenzbetrachtungen zum Stofftransport am Einzeltropfen—Validierung numerischer Ergebnisse, Chem. Ing. Tech. 73 (11) (2001) 1431–1435, English translation: Treatment of limits for the mass transfer at single droplets—validation of numerical results, Chem. Eng. Tech. 25(10) (2002) 953–956.

[13] W.H. Piarah, Numerische Untersuchung des instationaren Stofftransports an und in umstromten Einzeltropfen, Ph.D. Thesis, TU Berlin, Verlag Dr. Koster, Berlin, 2001.

[14] W.H. Piarah, A. Paschedag, M. Kraume, Numerical simulation of mass transfer between a single drop and an ambient flow, AIChE J. 47 (7) (2001) 1701–1704.

[15] U.J. Plöcker, H. Schmidt-Traub, Instationärer Stofftransport zwischen einer Einzelkugel und einer ruhenden Umgebung, Chem. Ing. Tech. 44 (1972) 313–319.

[16] M. Qi, H. Haverland, A. Vogelpohl, Auslegung von pulsierenden Siebboden- und Sprühkolonnen für die Extraktion auf der Basis von Einzeltropfenuntersuchungen, Chem. Ing. Tech. 72 (3) (2000) 203–314.

[17] A.R. Uribe-Ramirez, W.J. Korchinsky, Fundamental theory for prediction of single-component mass transfer in liquid drops at intermediate Reynolds numbers, Chem. Eng. Sci. 55 (2000) 3305–3318.